Measurement of the Quasifree $p + n \rightarrow d + \eta$ Reaction near Threshold

H. Calén, J. Dyring, K. Fransson, L. Gustafsson, S. Häggström, B. Höistad, A. Johansson, T. Johansson, S. Kullander, A. Mörtsell, R. J. M. Y. Ruber, U. Schuberth, and J. Zlomanczuk
Department of Radiation Sciences, Uppsala University, S-75121 Uppsala, Sweden

C. Ekström
The Svedberg Laboratory, S-75121 Uppsala, Sweden

K. Kilian, W. Oelert, V. Renken, and T. Sefzick
IKP, Forschungszentrum Jülich GmbH, D-52425 Jülich 1, Germany

A. Bondar, A. Kuzmin, B. Shwartz, V. Sidorov, and A. Sukhanov
Budker Institute of Nuclear Physics, Novosibirsk 630 090, Russia

A. Kupsc, P. Marciniewski, and J. Stepaniak
Institute for Nuclear Studies, PL-00681 Warsaw, Poland

V. Dunin, B. Morosov, A. Povtorejko, A. Sukhanov, and A. Zernov
Joint Institute for Nuclear Research, Dubna, 101000 Moscow, Russia

J. Zabierowski
Institute for Nuclear Studies, PL-90137 Lódz, Poland

Z. Wilhelmi
Institute of Experimental Physics, Warsaw University, PL-0061 Warsaw, Poland
(Received 14 April 1997)

The quasifree $p + n \rightarrow d + \eta$ reaction cross section has been measured in the near-threshold region using deuterium from an internal cluster-jet target and 1350 MeV protons in the CELSIUS storage ring of the The Svedberg Laboratory, Uppsala. The energy dependence of the cross section is extracted by exploiting the Fermi momentum of the target neutron and reconstructing the kinematics on an event-by-event basis. The data cover center of mass excess energies from 16 to 113 MeV. [S0031-9007(97)04165-3]

PACS numbers: 13.75.Cs, 14.20.Gk, 25.10.+s, 25.40.Ve

As more data are becoming available on η-meson production near the kinematical threshold, the interest in η-meson physics has increased considerably. In particular, attention has been given to the relatively strong and attractive S-wave η-nucleon interaction. The near-threshold region is appropriate for S-wave interaction studies since the final state involves primarily the lowest partial wave. Both the production mechanism and the η-N final state interaction are expected to be dominated by the presence of the N^* (1535) S_{11} resonance.

Precise η cross section data for nucleon-nucleon collisions are available only for the proton-proton reaction channel. It is therefore of interest to get complementary data from the neutron-proton channel. Such data will contribute to the understanding of the η production process, its isospin and spin dependence, and the importance of different meson exchanges. Available data for the neutron-proton channel are as yet very limited. Cross sections have been unfolded either from data obtained using the upper energy tail of a neutron beam [1] or from inclusive measurements using a proton beam on a deuterium target [2]. It is, however, evident from these data that the cross section for η production is significantly higher in $p + n$ than in $p + p$ collisions. In this paper we present the first measurement of the cross section for the quasifree $p + n \rightarrow d + \eta$ reaction using a deuterium target. The energy dependence is obtained by reconstructing the Fermi momentum of the neutron for the individual events.

The experiment was carried out at the CELSIUS storage ring of the The Svedberg Laboratory, Uppsala, using the WASA/PROMICE detector setup [3]. A circulating proton beam with a kinetic energy of $T_p = 1350$ MeV was brought to interact with an internal deuterium cluster-jet target. The integrated luminosity in the experiment was approximately 100 nb^{-1}. An η meson is identified by its 2γ decay [$B = (39.25 \pm 0.31)\%$ [4]] recorded in two arrays of CsI(Na) detectors placed at each side of the beam pipe. Each array is made from 56 tapered elements and covers polar angles between approximately 30°

 0031-9007/97/79(14)/2642(4)$10.00

and 90° and azimuthal angles between ±25°. Scintillator hodoscopes are placed in front of the arrays to veto charged particles. The 2γ invariant mass resolution obtained at the η-meson mass is 20 MeV (σ). Forward-going charged particles are measured in a detector system covering scattering angles between 4° and 22° with essentially full coverage of the azimuthal angles. This system consists of a tracking detector made from straw chambers, followed by a three-layer scintillator hodoscope and a four-layer calorimeter made from 11-cm-thick scintillators. Another scintillator hodoscope is placed at the end of the detector system to register penetrating particles. More details about the detector setup and its performance can be found in Ref. [3].

There are several reactions that contribute to η production in $p + d$ collisions at the incident proton energy of 1350 MeV:

$$p + d \rightarrow p + p + n_s + \eta\,, \quad (1)$$

$$\rightarrow p + n + p_s + \eta\,, \quad (2)$$

$$\rightarrow d + p_s + \eta\,, \quad (3)$$

$$\rightarrow p + d + \eta\,, \quad (4)$$

$$\rightarrow {}^3\mathrm{He} + \eta\,, \quad (5)$$

where the s subscript denotes a slow spectator nucleon for the dominant quasifree reactions. The cross sections for reactions (4) and (5) are small in comparison with reactions (1)–(3) and can safely be neglected in the analysis at the present level of precision [5,6]. Measuring the ηs as well as the other residual particles makes it possible to identify reactions (1)–(3) and to measure their cross sections.

The Fermi motion of the target nucleon affects the center of mass (CM) energy of the beam proton and the target nucleon on an event-by-event basis. Thus the CM energy may be extracted for each η event with a topology consistent with one of the reactions (1)–(3). This allows the energy dependence of the quasifree cross section to be measured using a fixed beam energy. The selection of η events is made using the information from the CsI(Na) detectors, and the reaction channel assignment is made using the additional information from the forward detectors.

For the interpretation of the data, extensive simulations have been carried out taking into account the geometry of the experiment and detector response using GEANT3 [7]. The Fermi momentum of the target nucleon has been included in the event generation using a parametrization of the deuteron wave function calculated from the Paris potential [8]. The results are sensitive only to Fermi momenta below 150 MeV/c.

The quasifree two-body final state $d + \eta$ is selected using kinematic constraints. The η energy-momentum 4-vector is reconstructed from the measured directions and energies of its two decay γ's and improved using a kinematical fit (1C). If the Fermi momentum of the target nucleon is neglected, the two-body kinematics makes it possible to predict the deuteron emission angle using only the η information. In Fig. 1(a) the differences between this calculated deuteron angle and the measured angle of the forward track are shown in spherical coordinates. A strong signal from the two-body $d + \eta$ process is seen in the region where the difference in polar and azimuthal angles is small. The points lying outside this region are compatible with what is expected from the three-body $(pN\eta)$ final states.

Figure 1(b) shows the distance between calculated and measured impact points in the tracking detector 90 cm downstream of the target. The data are shown together with distributions from the Monte Carlo simulation. The dashed and dotted lines correspond to the $d + \eta$ and the $p + N + \eta$ reactions, respectively, and the solid line to the sum of the two reactions. Phase space distributions

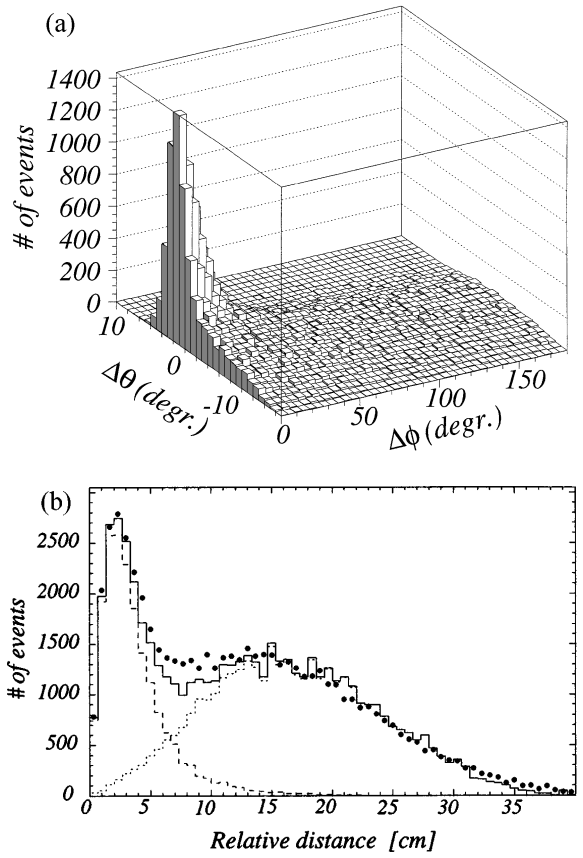

FIG. 1. (a) Lego plot showing the difference between predicted deuteron track using the measured η and free $p + n \rightarrow d + \eta$ kinematics and measured forward tracks in polar coordinates. True two-body events populate the $\Delta\theta = \Delta\phi = 0$ region where a clear signal is seen. The spread is due to the Fermi motion of the target neutron. (b) Distance between the calculated point of impact of a deuteron and the measured one for forward particles, at the position of the tracking detector, 90 cm downstream from the target. Superimposed are the results from an analysis using Monte Carlo data from the reactions $p + n \rightarrow d + \eta$ (dashed line), $p + N \rightarrow p + N + \eta$ (dotted line), and the sum of the two (solid line).

are used together with a parametrization of the measured shape of the $p + p + \eta$ cross section [9–11] for the $p + N + \eta$ channels. The experimental distribution is well described by these Monte Carlo data.

To provide a clean $d + \eta$ sample, only events at distances smaller than 5 cm in Fig. 1(b) are selected for further analysis. Figure 2 shows the distributions of the invariant 2γ mass for the selected events and for all events. A clean η peak is seen for the selected events, and the region of invariant masses used in the final analysis is indicated. The background from events with two uncorrelated γ's is 3% in this region. Simulations show that the contribution from the $p + n + \eta$ channel is about 10%, whereas the contribution from the $p + p + \eta$ channel, where one proton escapes undetected in the beam pipe, is negligible (<1%). The overall acceptance for the quasifree $p + n \rightarrow d + \eta$ reaction, including geometry and all cuts in the analysis, is a smooth function of the CM energy varying between 0.2% and 1%.

Knowing the direction of the deuteron, together with the energy and direction of the η meson, makes it possible to derive the Fermi momentum of the struck target neutron. The CM excess energy is then calculated $[Q_{\mathrm{CM}} = \sqrt{s} - (m_d + m_\eta)]$, on an event-by-event basis, assuming the spectator proton to be on its mass shell [12]. Simulations show that Q_{CM} can be reconstructed to an average precision of 5 MeV (σ) in this way.

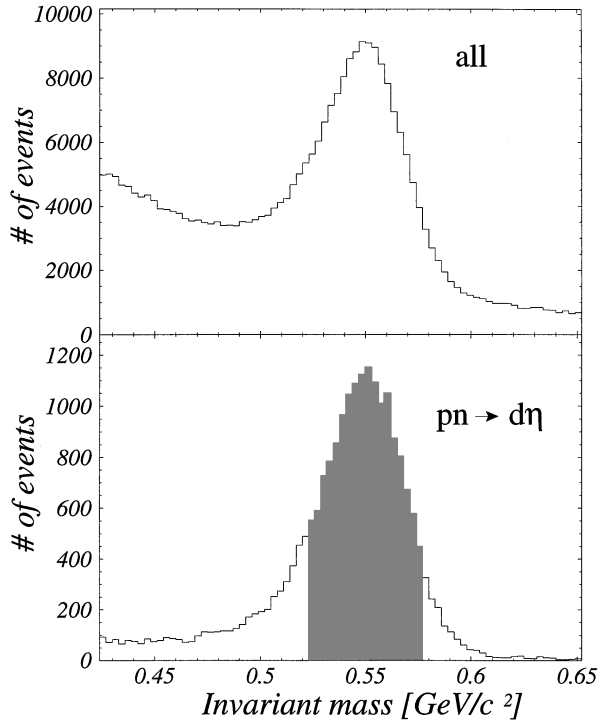

FIG. 2. Invariant 2γ mass distributions using the information from the two CsI(Na) arrays. The upper histogram corresponds to inclusive events. The lower histogram corresponds to the selected $p + n \rightarrow d + \eta$ candidate events shown in Fig. 1(b). The shaded area shows the region of invariant masses selected for the final analysis.

The normalization was established using quasielastic $p + p$ scattering data taken simultaneously with the η production data. By using the free elastic scattering cross section [13], no correction is needed for shadowing effects when relating the quasifree elastic and production processes. Any uncertainties are well within the quoted overall systematic error below. As a cross check of the normalization procedure, the quasifree reaction $p + p \rightarrow p + p + \eta$ was analyzed in a similar fashion using events with two charged forward-going tracks. In Fig. 3 the quasifree and the free reactions are compared, and they agree within errors in overlapping regions. Since this normalization has not been imposed, this gives additional confidence in the method used. Figure 3 also shows the energy dependence of the quasifree $p + n \rightarrow d + \eta$ cross section for Q_{CM} values between 16 and 113 MeV. Only statistical errors are shown. In addition, there are individual systematic errors for each data point and an overall uncertainty of 23% in the absolute normalization, the main source in the latter being the uncertainty in the $p + p$ quasielastic cross section [14]. As can be seen, the $p + n \rightarrow d + \eta$ cross section is substantially larger than the $p + p \rightarrow p + p + \eta$ cross section. Numerical values are given in Table I.

Figure 4 shows our measured cross section for the quasifree $p + n \rightarrow d + \eta$ reaction on a linear scale. The cross section increases from about 40 μb at the lowest energy up to 90 μb at Q_{CM} around 60 MeV. In this region, the shape essentially follows phase space (dotted curve), whereas for higher Q_{CM} values data start to deviate substantially from phase space. Also superimposed is a dashed curve which in addition to phase space includes a Breit-Wigner shape for the $N^*(1535)$ resonance in the

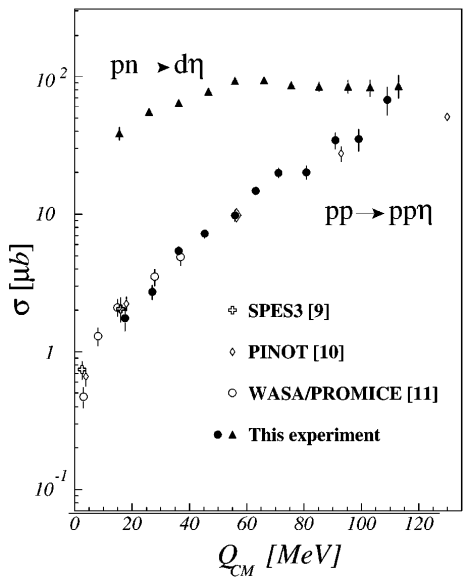

FIG. 3. Total cross sections for the quasifree $p + n \rightarrow d + \eta$ and $p + p \rightarrow p + p + \eta$ reactions (filled symbols) together with previously measured free reaction cross sections (open symbols) [9–11].

TABLE I. Total cross sections for the quasifree reaction $p + n \rightarrow d + \eta$. The errors given are statistical and systematic, respectively. In addition, there is an overall normalization error of 23%. The energy intervals correspond to the binning and the asymmetry is due to the weighting from the deuteron wave function.

CM excess energy [MeV]	Equivalent beam energy [MeV]	σ_{tot} [μb]
16^{+4}_{-6}	1289^{+11}_{-16}	$39 \pm 4 \pm 4$
26^{+4}_{-6}	1315^{+11}_{-15}	$56 \pm 3 \pm 3$
36^{+4}_{-6}	1341^{+11}_{-15}	$64 \pm 3 \pm 2$
47^{+3}_{-7}	1370^{+11}_{-18}	$77 \pm 3 \pm 2$
56^{+4}_{-6}	1394^{+11}_{-16}	$93 \pm 4 \pm 2$
66^{+4}_{-6}	1420^{+11}_{-15}	$94 \pm 5 \pm 2$
76^{+4}_{-6}	1447^{+11}_{-16}	$86 \pm 5 \pm 2$
85^{+5}_{-5}	1471^{+13}_{-13}	$85 \pm 7 \pm 2$
95^{+5}_{-5}	1498^{+13}_{-14}	$85 \pm 9 \pm 3$
103^{+7}_{-3}	1519^{+19}_{-8}	$83 \pm 12 \pm 3$
113^{+7}_{-3}	1546^{+19}_{-8}	$86 \pm 16 \pm 4$

η-N system [15]. The parameters of the resonance were obtained from electroproduction and photoproduction data near threshold as described in Ref. [16]. The shape of the experimental cross section then becomes well reproduced also for $Q_{\text{CM}} > 60$ MeV where the suppression is governed by the tail of the resonance. This result strongly suggests that the η production proceeds through the formation of an intermediate $N^*(1535)$ resonance.

Figure 4 also shows the Q_{CM} parametrization of the $p + n \rightarrow d + \eta$ cross section used in Ref. [1]. It is valid for values of Q_{CM} below our measured range and gives a sharp peak with a substantially larger cross section compared to an extrapolation of our measured values. It would be interesting to have more data in the region below $Q_{\text{CM}} < 15$ MeV to see whether or not the cross section increases very close to threshold, as suggested by the data of Ref. [1]. If confirmed, this increase would be evidence for a quasibound system formed by an η and the two nucleons [17–19].

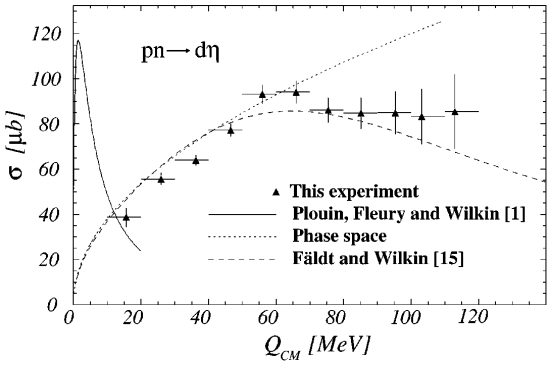

FIG. 4. The measured energy dependence of the quasifree $p + n \rightarrow d + \eta$ reaction. Also shown is a phase-space curve (dotted line) and a curve including both phase space and a Breit-Wigner shape representing the $N^*(1535)$ [15]. Both curves are arbitrarily normalized. Also included is the parametrization of the cross section from Ref. [1] in the very vicinity of the threshold (solid line).

In conclusion, we report on the first measurement of the energy dependence of the quasifree $p + n \rightarrow d + \eta$ reaction near threshold. This was made possible by analyzing η production from quasifree $p + n$ interactions using a D_2 target and exploiting the Fermi momentum of the target neutron. The shape of the energy dependence is reproduced by a calculation taking into account phase space and the $N^*(1535)$ resonance, showing the first experimental indication of the importance of this S_{11} resonance for nucleon induced reactions. The data presented will constrain existing models [17,20,21] and provide new input to theoretical efforts in this field.

We are grateful to the personnel at the The Svedberg Laboratory and the Department of Radiation Sciences for their cooperation and skillful work during the course of this experiment. Special thanks are due C. Wilkin and G. Fäldt for encouragement and numerous fruitful discussions. The financial support from the Swedish Natural Science Research Council, the Swedish Royal Academy of Sciences, the Swedish Institute, the Polish State Committee for Scientific Research (KBN No. 2P03B07910), and the Russian Academy of Sciences is gratefully acknowledged.

[1] F. Plouin, P. Fleury, and C. Wilkin, Phys. Rev. Lett. **65**, 690 (1990).
[2] E. Chiavassa *et al.*, Phys. Lett. B **337**, 192 (1994).
[3] H. Calén *et al.*, Nucl. Instrum. Methods Phys. Res., Sect. A **379**, 57 (1996).
[4] R. M. Barnett *et al.*, Phys. Rev. D **53**, 1 (1996).
[5] U. Tengblad, Internal Report No. TSL/ISV-96-0163.
[6] J. Banaigs *et al.*, Phys. Lett. **45B**, 394 (1973).
[7] R. Brun *et al.*, GEANT3, CERN Report No. DD/EE/84-1, 1987.
[8] M. Lacombe *et al.*, Phys. Lett. **101B**, 139 (1981).
[9] A. M. Bergdolt *et al.*, Phys. Rev. D **48**, 2969 (1993).
[10] E. Chiavassa *et al.*, Phys. Lett. B **322**, 270 (1994).
[11] H. Calén *et al.*, Phys. Lett. B **366**, 39 (1996).
[12] P. Benz *et al.*, Nucl. Phys. **B65**, 158 (1973).
[13] R. A. Arndt, I. I. Strakovsky, and R. L. Workman, Phys. Rev. C **50**, 2731 (1994).
[14] S. Häggström, Ph.D. thesis, Uppsala University, Acta Universitatis Upsaliensis 13, 1997.
[15] G. Fäldt and C. Wilkin (private communication).
[16] G. Fäldt and C. Wilkin, Nucl. Phys. **A587**, 769 (1995).
[17] T. Ueda, Phys. Rev. Lett. **66**, 297 (1991).
[18] S. A. Rakityansky *et al.*, Phys. Rev. C **53**, 2043 (1996).
[19] A. M. Green, J. A. Niskanen, and S. Wycech, Phys. Lett. B **394**, 253 (1996).
[20] J. M. Laget, F. Wellers, and J. F. Lecolley, Phys. Lett. B **257**, 254 (1991).
[21] A. Moalem *et al.*, Nucl. Phys. **A600**, 445 (1996).